

# Stabilizing a Weak Binding State for Effectors in the Human Ras Protein by Cyclen Complexes\*\*

Ina C. Rosnizeck, Thorsten Graf, Michael Spoerner, Jens Tränkle, Daniel Filchtinski, Christian Herrmann, Lothar Gremer, Ingrid R. Vetter, Alfred Wittinghofer, Burkhard König, and Hans Robert Kalbitzer\*

The guanine nucleotide binding (GNB) protein Ras is involved in cellular signal transduction pathways that induce proliferation, differentiation, and apoptosis of cells. It functions as a molecular switch, cycling between an inactive GDP-bound state and an active GTP-bound state. Only Ras complexed with GTP is able to bind different effectors such as Raf kinase or RalGDS with high affinity (see, for example, Ref. [1]).  $^{31}\text{P}$  NMR spectroscopy has revealed the existence of at least two distinct conformational states, which are in dynamic equilibrium, when wild-type Ras is bound to the GTP analogues GppNHp or GppCH<sub>2</sub>p.<sup>[2,3]</sup> State 1 is recognized by guanine nucleotide exchange factors (GEFs),<sup>[4]</sup> state 2 by effector proteins.<sup>[2,3,5–9]</sup> The affinity of state 1 for effectors is smaller by a factor of approximately 20.<sup>[7]</sup> Thus state 1 represents a weak binding state for effectors. In more than 30 % of all human cancers Ras is found mutated at amino acid position 12, 13, or 61.<sup>[10]</sup> In the cell, these mutants are locked in the active GTP-bound state owing to their loss of intrinsic as well as GAP (GTPase activating protein) accel-

erated GTP hydrolysis. It should be possible to interrupt the effector interaction of activated, GTP-bound oncogenic Ras by suitable small compounds that selectively stabilize state 1. As shown by  $^{31}\text{P}$  NMR spectroscopy, the zinc(II) complex of 1,4,7,10-tetraazacyclododecane complex ( $\text{Zn}^{2+}$  cyclen; Figure S1 in the Supporting Information) selectively binds to the conformational state 1 of activated Ras and thus shifts the dynamic equilibrium of activated Ras towards the weak binding state.<sup>[11,12]</sup> As a precondition for using  $\text{Zn}^{2+}$  cyclen as lead structure for the structure-based development of inhibitors of the Ras-effector interaction, a three-dimensional structure of the complex is required, and this is presented here.

$\text{Cu}^{2+}$  cyclen, which can be used as a paramagnetic analogue of  $\text{Zn}^{2+}$  cyclen, induces distance-dependent nuclear relaxation in the nearby nuclei of the protein. Figure 1 (spectrum A) shows the  $^{31}\text{P}$  NMR spectrum of Ras(wt)- $\text{Mg}^{2+}$ -GppNHp, which is characteristic for the simultaneous existence of the two conformational states 1 and 2 ( $K_{12} = [2]/[1] = 1.9$ ) since two sets of resonance lines for the

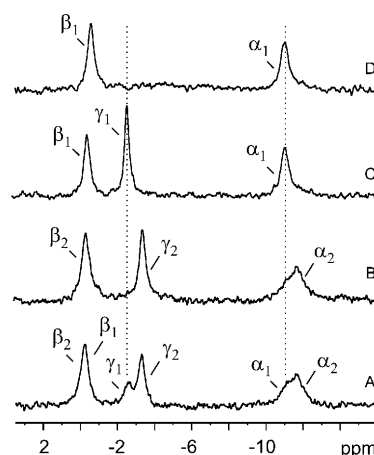


**Figure 1.**  $\text{Cu}^{2+}$  cyclen and its influence on  $^{31}\text{P}$  NMR spectra of Ras-GppNHp complexes.  $^{31}\text{P}$  NMR spectrum of Ras- $\text{Mg}^{2+}$ -GppNHp in 40 mM Tris/HCl, pH 7.5, 10 mM  $\text{MgCl}_2$ , 2 mM dithioerythrol (DTE), 0.2 mM 4,4-dimethyl-4-silapentane-1-sulfonic acid (DSS), and 5 %  $\text{D}_2\text{O}$ . A) 1.3 mM Ras(wt)- $\text{Mg}^{2+}$ -GppNHp, B) 1.3 mM Ras(wt)- $\text{Mg}^{2+}$ -GppNHp in the presence of 2.6 mM of  $\text{Cu}^{2+}$  cyclen, C) 1.3 mM Ras-(T35A)- $\text{Mg}^{2+}$ -GppNHp, and D) 1.3 mM Ras-(T35A)- $\text{Mg}^{2+}$ -GppNHp in the presence of 6.5 mM of  $\text{Cu}^{2+}$  cyclen.  $\alpha_1$ ,  $\beta_1$ ,  $\gamma_1$ ,  $\alpha_2$ ,  $\beta_2$ ,  $\gamma_2$ : resonances of the  $\alpha$ -,  $\beta$ -, and  $\gamma$ -phosphate groups in state 1 and state 2, respectively. The peaks corresponding to the state 1 conformation are marked with dashed lines. All spectra were recorded at 278 K and 202 MHz.

[\*] I. C. Rosnizeck, T. Graf, M. Spoerner, Prof. H. R. Kalbitzer  
Universität Regensburg

Institut für Biophysik und Physikalische Biochemie  
Universitätsstrasse 31, 93053 Regensburg (Germany)  
E-mail: hans-robert.kalbitzer@biologie.uni-regensburg.de

J. Tränkle, D. Filchtinski, C. Herrmann  
Ruhr-Universität Bochum, Institut für Physikalische Chemie I  
Universitätsstrasse 150, 44780 Bochum (Germany)

L. Gremer,<sup>[†]</sup> I. R. Vetter, A. Wittinghofer  
Max Planck Institut für Molekulare Physiologie  
Abteilung Strukturelle Biologie  
Otto-Hahn Strasse 11, 44227 Dortmund (Germany)

B. König  
Universität Regensburg, Institut für Organische Chemie  
Universitätsstrasse 31, 93053 Regensburg (Germany)

[†] Current address:  
Klinikum der Heinrich-Heine-Universität Düsseldorf  
Institut für Biochemie und Molekularbiologie II  
Universitätsstrasse 1, 40225 Düsseldorf (Germany)

[\*\*] This research was supported by the Deutsche Forschungsgemeinschaft, the Fonds der Chemischen Industrie, and the Volkswagenstiftung. We thank the beamline staff of X10SA at the Swiss Light Source Paul Scherrer Institute, Villigen (Switzerland), for support and our colleagues of MPI Dortmund (Michael Weyand, Katja Gotthardt, and Antje Schulte) for help with the data collection. We also thank Michael Kruppa and Florian Schmidt for the synthesis of the transition-metal cyclen complexes.

Supporting information for this article is available on the WWW under <http://dx.doi.org/10.1002/anie.200907002>.

bound nucleotide are observed. In the presence of  $\text{Cu}^{2+}$  cyclen the  $^{31}\text{P}$  resonances of the  $\beta$ - and  $\gamma$ -phosphate corresponding to state 1 shift upfield, with the stronger effect observed for the  $\gamma$ -phosphate group; in contrast, the signal of the  $\alpha$ -phosphate shifts slightly downfield. Simultaneously, with increasing concentrations of  $\text{Cu}^{2+}$  cyclen the lines broaden. At a ligand/protein ratio of more than 2:1 the  $\gamma$ -phosphate line has already broadened beyond detection and the  $\beta$ -phosphate line is slightly broadened (Figure 1). The resonances belonging to state 2 are not affected by addition of  $\text{Cu}^{2+}$  cyclen; that is, they are neither shifted nor broadened at this  $\text{Cu}^{2+}$  cyclen concentration. As an independent control the same experiments were performed with Ras-(T35A)- $\text{Mg}^{2+}$ -GppNHp, which exists predominantly in the conformational state 1 ( $K_{12} < 0.1$ ). Here the effects of the  $\text{Cu}^{2+}$  cyclen binding can be observed more easily because the signals belonging to state 2 are virtually absent. Again the resonance signal of the  $\gamma$ -phosphate becomes broadened and completely disappears at a  $\text{Cu}^{2+}$  cyclen/Ras ratio of 2:1 (Figure 1, spectra C and D). These data indicate that the  $\text{Cu}^{2+}$  cyclen binds close to the  $\gamma$ -phosphate of GppNHp in state 1 of Ras but does not recognize the active site of the protein in state 2. Since Ras(T35A) exists predominantly in state 1, it was used in the further structural investigation of the binding of cyclen-metal complexes to Ras in conformational state 1.

The distance from the  $\text{Cu}^{2+}$  ion to the phosphorus nuclei of the bound GppNHp can be estimated from the paramagnetic enhancement of the relaxation times as  $(0.30 \pm 0.05)$ ,  $(0.48 \pm 0.05)$ , and  $(0.54 \pm 0.05)$  nm for the  $\gamma$ -,  $\beta$ -, and  $\alpha$ -phosphate groups, respectively (see Table S1 in the Supporting Information). It is very likely that the positively charged  $\text{Cu}^{2+}$  cyclen that is almost within van der Waals distance to the negatively charged  $\gamma$ -phosphate group is directly bound to an oxygen atom of the  $\gamma$ -phosphate group. In crystal structures of a corresponding  $\text{Zn}^{2+}$  cyclen derivative in a 1:1 complex with phenylphosphate,<sup>[13]</sup> the  $\text{Zn}^{2+}$  ion is separated from the phosphorus nucleus by 0.294 nm.

Addition of the paramagnetic  $\text{Cu}^{2+}$  cyclen leads to a reduction of crosspeak intensities in the  $^{1}\text{H}$ ,  $^{15}\text{N}$  HSQC NMR spectra as well as to changes of chemical shifts (see Table S2 and Figure S2 in the Supporting Information). The signal intensities of the resonances of Gly13, located in the P-loop close to the  $\gamma$ -phosphate group of the bound nucleotide, and of Gly60, located in switch II decrease substantially, and they completely disappear at higher concentrations of  $\text{Cu}^{2+}$  cyclen. Other resonances, for example, those of Ser118 or Thr148, are not perturbed by addition of  $\text{Cu}^{2+}$  cyclen. The addition of the diamagnetic compound  $\text{Zn}^{2+}$  cyclen to the sample leaves most of the resonances unperturbed, but some resonances are shifted and/or broadened. Most interestingly, a number of resonances are split into two lines, for example, the resonances that correspond to Ile124 and Gly115 (see Table S2 and Figure S2 in the Supporting Information).

Highlighting the residues with values of the combined chemical-shift changes  $\Delta\delta^{\text{comb}} \geq \sigma_0^{\text{corr}}$  on the surface of the crystal structure of Ras(wt) reveals two distinct sites (Figure 2). An analysis of the concentration dependence of the chemical-shift changes confirms the existence of two sites,

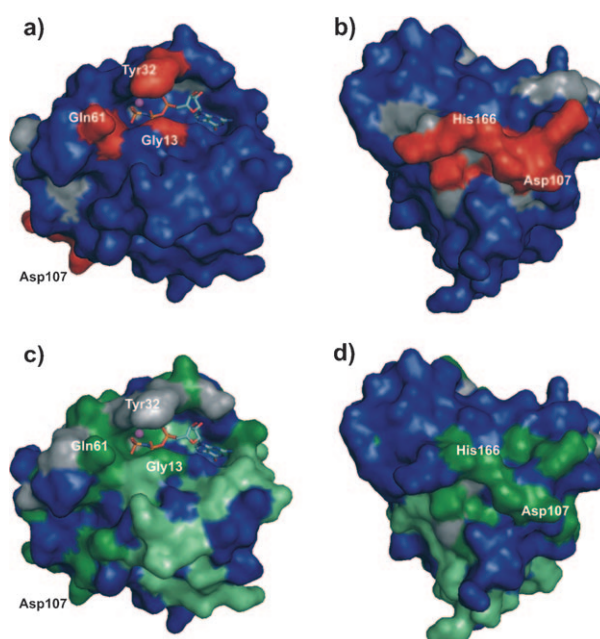


**Figure 2.** Binding sites for  $\text{Zn}^{2+}$  and  $\text{Cu}^{2+}$  cyclen in Ras- $\text{Mg}^{2+}$ -GppNHp as determined by  $^{1}\text{H}$ ,  $^{15}\text{N}$  HSQC NMR spectroscopy. a,b) Amino acids clearly affected by the paramagnetic distance-dependent  $\text{Cu}^{2+}$  effect mapped onto the surface of Ras(wt)- $\text{Mg}^{2+}$ -GppNHp.<sup>[16]</sup> Residues exhibiting a significant relative signal reduction  $I(j)/I_0(j) < 1 - \sigma_0$  are in red, not clearly assignable residues are in gray. c,d) Amino acids showing significant shift perturbations in the presence of  $\text{Zn}^{2+}$  cyclen mapped onto the surface of Ras(wt)- $\text{Mg}^{2+}$ -GppNHp; dark green: residues with a significant combined chemical-shift change  $\Delta\delta^{\text{comb}} \geq \sigma_0^{\text{corr}}$ , light green: residues showing a line splitting upon binding of  $\text{Zn}^{2+}$  cyclen typical for a slow-exchange process, gray: not clearly assignable residues.

one site where half-saturation is reached at a ligand concentration of approximately 2 mM and another class where half-saturation is observed at a ligand concentration of approximately 6 mM. Since we also have data from the paramagnetic analogue  $\text{Cu}^{2+}$  cyclen, long-range structural effects on chemical shifts from ligand binding can be recognized because of the strong distance dependence of the paramagnetic relaxation enhancement (PRE). Binding site 1 (Figure 2a,c) is close to the  $\gamma$ -phosphate of the nucleotide in accordance to the  $^{31}\text{P}$  NMR data. The residues most affected are Gly13, Tyr32, Ala59, Gly60, and Gln61, which are located in the P-loop (amino acids 10–18), the PM3 motif (57–61), and in switch II (60–72). The second binding site (Figure 2b,d) in the negatively charged loop L7 comprises Asp105, Ser106, Asp107, Asp108, Val109, and Met111, and residues near the C terminus—Glu162, Gln165, and His166.

The chemical-shift perturbation data and the distance restraints obtained from the paramagnetic relaxation enhancement were used to calculate (program HADDOCK) the structure of the protein with the cyclen ligand at binding site 1.<sup>[14,15]</sup> Because of the lack of an X-ray structure of Ras(T35A)- $\text{Mg}^{2+}$ -GppNHp, for the structure calculation the crystal structure of Ras(wt)- $\text{Mg}^{2+}$ -GppNHp<sup>[16]</sup> was modified by replacing threonine 35 by alanine. The crystal structure of the wild-type protein is assumed to represent state 2, whereas

Ras(T35A) and Ras(T35S) bound to  $\text{Mg}^{2+}$ -GppNHp are predominantly in state 1. The available X-ray structure of Ras(T35S)- $\text{Mg}^{2+}$ -GppNHp<sup>[7]</sup> was used to derive distance restraints for the nucleotide and the  $\text{Mg}^{2+}$  ion in the structure calculation (for details of the calculation see Table S3 in the Supporting Information).

In Figure 3 a surface plot of the Ras(wt) structure as well as the lowest energy structure obtained from the HADDOCK calculations is depicted. The  $\text{Cu}^{2+}$  cyclen complex is bound to

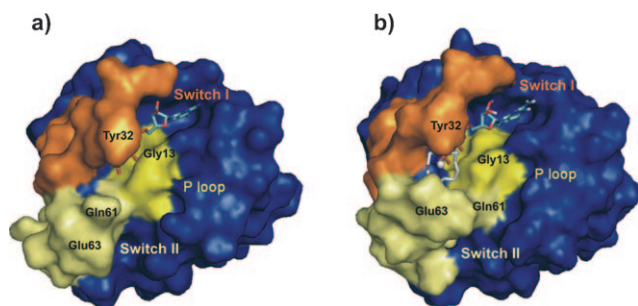


**Figure 3.** Comparison of the calculated structure of Ras-(T35A)- $\text{Mg}^{2+}$ -GppNHp complexed with  $\text{Cu}^{2+}$  cyclen and the X-ray structure of wild-type Ras. a) Surface representation of the X-ray structure of Ras(wt)- $\text{Mg}^{2+}$ -GppNHp<sup>[6]</sup> (pdb 5p21). b) Surface plot of the HADDOCK structure of Ras(T35A)- $\text{Mg}^{2+}$ -GppNHp complexed with  $\text{Cu}^{2+}$  cyclen (white). The switch regions and the phosphate-binding loop are in orange, light yellow, and yellow, respectively.

the  $\gamma$ -phosphate of GppNHp by means of its metal center; the four amine protons of the cyclen moiety are in hydrogen-bonding distances to the carbonyl oxygens of Gly12, Asp33, Ala35, and Ala59. Such a hydrogen-bonding pattern could also explain the strong shifts of the signals of the neighboring amino acids Gly13, Ile36, and Gly60 after binding of  $\text{Zn}^{2+}$  cyclen. The obtained interaction energies of  $\text{Cu}^{2+}$  cyclen with the protein are in a reasonable range (see Table S4 in the Supporting Information). The general topology of the Ras protein is unchanged, as expected.

The backbone root mean square deviation (RMSD) between the NMR structure of Ras(T35A)- $\text{Mg}^{2+}$ -GppNHp complexed with  $\text{Cu}^{2+}$  cyclen and the crystal structure of Ras(wt)- $\text{Mg}^{2+}$ -GppNHp<sup>[16]</sup> is 0.12 nm (see Figure S3 in the Supporting Information). The two structures show good agreement in the regions that should be similar in state 1 and state 2. However, significant conformational changes are observed. While switch I and the P loop adopt a more opened conformation, switch II moves towards the nucleotide binding site. A similar structural pattern is found in the crystal structure of the complex between Ras and its exchange factor SOS.<sup>[17]</sup> In our calculated structure Tyr32 is rotated and has turned away from the Ras-bound nucleotide. A change of the position of Tyr32 was already postulated by Geyer et al.<sup>[2]</sup> as a explanation of the  $^{31}\text{P}$  NMR shift differences between state 1 and state 2 of the Ras protein. Hall et al.<sup>[18]</sup> could also show that the Tyr32 is no longer in its position in state 2 in the structure of the Ras(A59G) mutant. In addition, Glu63 moves towards the nucleotide-binding site and His27 seems to change its position. In general, the cleft containing the

nucleotide is more open in state 1 than in state 2, which is in accordance with the observed preference of the guanine exchange factor SOS for state 1.<sup>[4]</sup> It also explains the measured decrease of the partial molar volume after transition from state 2 to state 1,<sup>[4]</sup> since a decrease of the partial volume is usually associated with an increase of the surface exposed to water.

Additionally, we solved the crystal structure of Ras(wt)- $\text{Mg}^{2+}$ -GppNHp complexed to  $\text{Zn}^{2+}$  cyclen with a resolution of 2.1 Å (see Table S5 in the Supporting Information). The obtained structure is depicted in Figure 4a.

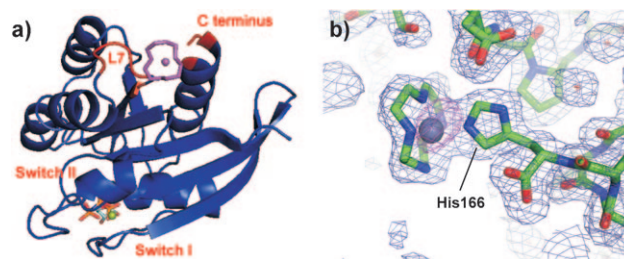


**Figure 4.** Crystal structure of Ras(wt)-GppNHp complexed to  $\text{Zn}^{2+}$  cyclen. a) Ribbon plot of the crystal structure of wild-type Ras- $\text{Mg}^{2+}$ -GppNHp complexed to  $\text{Zn}^{2+}$  cyclen (magenta). The residues identified as belonging to the second binding site by NMR paramagnetic relaxation enhancement studies with  $\text{Cu}^{2+}$  cyclen are in red. b) Electron density map for the coordination of  $\text{Zn}^{2+}$  cyclen to Ras(wt)- $\text{Mg}^{2+}$ -GppNHp.

$\text{Zn}^{2+}$  cyclen can be detected only at binding site 2, which was already identified in the NMR studies and is located close to the C terminus and loop L7. The  $\text{Zn}^{2+}$  ion is coordinated to an imidazole nitrogen of the side chain of the C-terminal histidine 166 (Figure 4b). The protein itself is essentially unaltered except around the switch II region from amino acids 62 to 75 (RMSD of 0.241 nm for the 14 residues); here the density is not very well defined, as is common in Ras structures. In addition, the loop around residue 106 is somewhat shifted relative to the apo structure (RMSD 0.024 nm for 14 residues from residues 96 to 109). The crystal structures of wild-type Ras- $\text{Mg}^{2+}$ -GppNHp determined here before and after treatment with  $\text{Zn}^{2+}$  cyclen showed the switch I region in very similar conformations. However, in these structures switch I is slightly more closed than in the structure reported by Pai et al.,<sup>[16]</sup> which crystallized in a different space group. In the crystals analyzed in this work, the molecules pack by means of the effector loops (in the state 2 conformation) which lie face to face next to each other. The affinity of  $\text{Zn}^{2+}$  cyclen at the concentration used for the incubations (25 mM) was apparently too low to overcome the force that holds the effector loop shut by the  $\gamma$ -phosphate together with the crystal packing forces, otherwise the crystals would have cracked. Thus we did not expect to see any  $\text{Zn}^{2+}$  cyclen complex at site 1 in the crystal structure.

Both cyclen-metal complexes favor the weak binding state of active Ras. Since state 1 is assumed to be a weak effector-binding state, the cyclen transition-metal complexes are expected to impair effector binding to active Ras by



stabilization of the weak binding state. To confirm this assumption, Ras/Raf binding was measured by isothermal titration calorimetry in the presence of cyclens (Figure 5). As proposed, the binding of the Ras binding domain of Raf

shows. Thus  $\text{Zn}^{2+}$  cyclen can serve as a lead compound for a novel approach for inhibiting the Ras–effector interaction.

### Experimental Section

Details of the protein purification, the NMR spectroscopy, the X-ray crystallography, the evaluation of the chemical shift changes and the paramagnetic relaxation enhancement induced by ligand binding, the NMR structure calculation, and the calorimetry are given as Supporting Information.

Received: December 12, 2009

Published online: April 16, 2010

**Keywords:** cyclen · drug design · NMR spectroscopy · Ras protein · signal transduction

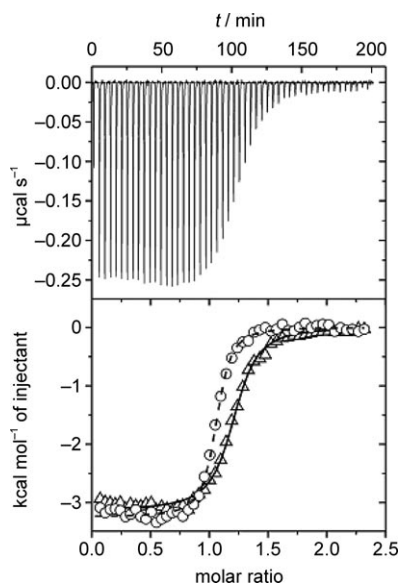


**Figure 5.** Perturbation of the Ras/Raf interaction by  $\text{Zn}^{2+}$  cyclen. ITC measurements were performed at 298 K with a sample containing 40  $\mu\text{M}$  H-Ras(wt)- $\text{Mg}^{2+}$ -GppNHp in 50 mM Tris/HCl pH 7.5, 100 mM NaCl, 5 mM  $\text{MgCl}_2$ , 2 mM DTE. The sample was titrated with a 400  $\mu\text{M}$  solution of Raf-RBD (Ras-binding domain of Raf) in the same buffer in the absence (○) and in the presence of 1–10 mM  $\text{Zn}^{2+}$  cyclen (Δ, data depicted for 4 mM  $\text{Zn}^{2+}$  cyclen), respectively. The heating power of the latter titration is shown as a function of time (upper panel). The change of enthalpy is plotted as a function of the molar ratio of Raf to Ras. Data are fitted with a 1:1 binding model.

kinase to Ras(wt)-GppNHp is perturbed in the presence of either  $\text{Zn}^{2+}$  cyclen or  $\text{Cu}^{2+}$  cyclen, leading to a decreased apparent affinity between Ras and Raf.

In conclusion,  $\text{Zn}^{2+}$  cyclen and  $\text{Cu}^{2+}$  cyclen complexes bind to two spatially separated sites in Ras- $\text{Mg}^{2+}$ -GppNHp with millimolar affinity. The binding site responsible for selective stabilization of the conformational state 1 with decreased effector affinity is close to the  $\gamma$ -phosphate of the bound nucleotide in active Ras. An analogous binding site close to the phosphate moieties cannot be found in Ras- $\text{Mg}^{2+}$ -GDP as shown by  $^{31}\text{P}$  NMR studies (data not shown). Binding of  $\text{Zn}^{2+}$  cyclen opens the nucleotide-binding cleft and simultaneously decreases the effector affinity as the isothermal titration calorimetry of the complex with RafRBD

- [1] A. Wittinghofer, H. Waldmann, *Angew. Chem.* **2000**, *112*, 4360; *Angew. Chem. Int. Ed.* **2000**, *39*, 4192.
- [2] M. Geyer, T. Schweins, C. Herrmann, T. Prisner, A. Wittinghofer, H. R. Kalbitzer, *Biochemistry* **1996**, *35*, 10308.
- [3] M. Spoerner, A. Nuehs, P. Ganser, C. Herrmann, A. Wittinghofer, H. R. Kalbitzer, *Biochemistry* **2005**, *44*, 2225.
- [4] H. R. Kalbitzer, M. Spoerner, P. Ganser, C. Hosza, W. Kremer, *J. Am. Chem. Soc.* **2009**, *131*, 16714.
- [5] M. Geyer, C. Herrmann, S. Wohlgemuth, A. Wittinghofer, H. R. Kalbitzer, *Nat. Struct. Biol.* **1997**, *4*, 694.
- [6] T. Linnemann, M. Geyer, B. K. Jaitner, C. Block, H. R. Kalbitzer, A. Wittinghofer, C. Herrmann, *J. Biol. Chem.* **1999**, *274*, 13556.
- [7] M. Spoerner, C. Herrmann, I. R. Vetter, H. R. Kalbitzer, A. Wittinghofer, *Proc. Natl. Acad. Sci. USA* **2001**, *98*, 4944.
- [8] M. Spoerner, A. Wittinghofer, H. R. Kalbitzer, *FEBS Lett.* **2004**, *578*, 305.
- [9] W. Gronwald, F. Huber, P. Grunewald, M. Spörner, S. Wohlgemuth, C. Herrmann, A. Wittinghofer, H. R. Kalbitzer, *Structure* **2001**, *9*, 1029.
- [10] J. Bos, *Cancer Res.* **1989**, *49*, 4682.
- [11] H. R. Kalbitzer, B. Koenig, WO 2004006934, **2004**, A2 20040122, CAN 140:122769, AN 2004:60322.
- [12] M. Spoerner, T. Graf, B. König, H. R. Kalbitzer, *Biochem. Biophys. Res. Commun.* **2005**, *334*, 709.
- [13] S. Aoki, K. Iwaida, N. Hanamoto, M. Shiro, E. Kinura, *J. Am. Chem. Soc.* **2002**, *124*, 5256–5257.
- [14] C. Dominguez, R. Boelens, A. M. J. J. Bonvin, *J. Am. Chem. Soc.* **2003**, *125*, 1731.
- [15] A. D. J. van Dijk, R. Boelens, A. M. J. J. Bonvin, *FEBS J.* **2005**, *272*, 293.
- [16] E. F. Pai, U. Krengel, G. A. Petsko, R. S. Goody, W. Kabsch, A. Wittinghofer, *EMBO J.* **1990**, *9*, 2351.
- [17] P. A. Boriack-Sjodin, S. M. Margarit, D. Bar-Sagi, J. Kuriyan, *Nature* **1998**, *394*, 337.
- [18] B. E. Hall, D. Bar-Sagi, N. Nassar, *Proc. Natl. Acad. Sci. USA* **2002**, *99*, 12138.